Modeling the effect of dust on the plasma parameters in a dusty argon discharge under microgravity

M. R. Akdim and W. J. Goedheer*
FOM-Institute for Plasmaphysics, Rijnhuizen, P.O. Box 1207, 3430-BE Nieuwegein, The Netherlands
(Received 18 December 2002; published 27 June 2003)

A dusty radio-frequency argon discharge is simulated with the use of a two-dimensional fluid model. In the model, discharge quantities, such as the fluxes, densities, and electric field are calculated self-consistently. The charge and density of the dust are calculated with an iterative method. During the transport of the dust, its charge is kept constant in time. The dust influences the electric potential distribution through its charge and the density of the plasma through recombination of positive ions and electrons on its surface. Results are presented for situations in which the dust significantly changes the discharge characteristics, both by a strong reduction of the electron density and by altering the electric potential by its charge. Simulations for dust particles having a radius of 7.5 μm show that a double space charge layer is created around the sharp boundary of the dust crystal. A central dust-free region (void) is created by the ion drag force. Inside this void a strong increase of the production of argon metastables is found. This phenomenon is in agreement with experimental observations, where an enhanced light emission is seen inside the void.

DOI: 10.1103/PhysRevE.67.066407 PACS number(s): 52.65.−y, 52.25.Vy, 52.27.Lw

I. INTRODUCTION

Plasma crystal experiments performed under microgravity conditions have shown dust particles that arrange in a crystal-like structure. In their plasmakristall experiment (PKE), chamber Morfill and co-workers [1,2] usually observed a stable void with two dust vortices near the edges of the electrodes. Also, an increase of light emission emerging from the center of the discharge has been observed.

Theoretical and numerical studies up to now have basically followed dust particles in the electric field and particle fluxes of an undisturbed discharge. An important aspect not covered is the influence of the dust on the discharge. For this, a fully self-consistent model is needed. We have developed such a model for dust containing radio-frequency (rf) discharge in argon and used it to investigate the behavior of dust particles. The model contains a dust fluid part which has been described briefly in Ref. [3]. In existing models [4–6], the influence of the dust particles on the discharge due to recombination on their surface or the motion of the dust as a fluid is neglected. In case discharges contain a considerable amount of dust, as in the PKE experiments, this approximation is not correct. Our model accounts for the influence of the dust fluid on the plasma and for its transport as a fluid. This makes it a sophisticated tool to study dusty discharges. In this paper we describe the results obtained with the argon-dust fluid model, studying, in particular, the dust-plasma interaction.

II. DESCRIPTION OF THE MODEL

A. Fluid model for the plasma species

To model the dynamics of a dusty plasma, we have used an extension of a previously described two-dimensional model [7], of which only the most important aspects will be summarized here. It consists of particle balance equations for the different species (electrons, ions, and metastables) and an energy balance equation for electrons. Ion-neutral collisions have been included to simulate a possible gas heating mechanism. For this we have used a simple approximation by assuming that the energy taken up from the electric field by the ions is dissipated locally in collisions with the gas [8]. This gas heating mechanism has been refined by taking the heating of the dust particle surface into account [9,10]. The dust particle (surface) temperature can affect the gas temperature, which, in turn, could affect the other elementary processes in the discharge.

In the model the density balance for each species j is

$$\frac{dn_j}{dt} + \vec{\nabla} \cdot \vec{\Gamma}_j = S_j , \tag{1}$$

where n_j is the particle's density, $\vec{\Gamma}_j$ is the flux of the species, and S_j is the local sink or source.

The momentum balance is replaced by the drift-diffusion approximation, where the particle flux consists of a diffusive term and a drift term,

$$\vec{\Gamma}_j = \mu_j n_j \vec{E} - D_j \vec{\nabla} n_j , \tag{2}$$

with μ_j and D_j being the mobility and diffusion coefficient of species j. $\vec{E}$ is the electric field.

For ions the characteristic momentum transfer frequency is only a few megahertz. To use the drift-diffusion approximation for ions for rf frequencies higher than a few megahertz the electric field in Eq. (2) is replaced by an effective electric field. Using this effective electric field $\vec{E}_{eff}$, inertia effects are taken into account. An expression for the effective electric field is obtained by neglecting the diffusive transport and inserting expression $\vec{\Gamma}_i = \mu_i n_i \vec{E}_{eff}$ in the simplified momentum balance

*Electronic address: goedheer@rijnh.nl

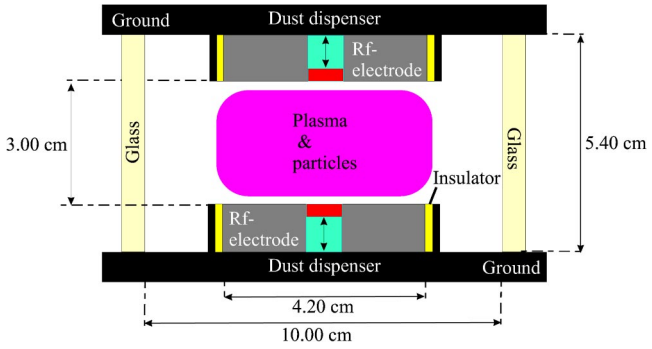

FIG. 1. Schematic diagram of the PKE reactor.

$$\frac{d\vec{\Gamma}_i}{dt} = \frac{en_i}{m_i}\vec{E} - \nu_{m,i}\vec{\Gamma}_i, \tag{3}$$

where $\nu_{m,i}$ is the momentum transfer frequency of the argon ions and is given by

$$\nu_{m,i} = \frac{e}{\mu_i m_i}. \tag{4}$$

Here e is the elementary charge and m_i is the mass of the argon ion. The effective electric field is then obtained by solving

$$\frac{d\vec{E}_{eff,i}}{dt} = \nu_{m,i}(\vec{E} - \vec{E}_{eff,i}). \tag{5}$$

The electric field $\vec{E}$ and potential V are calculated using the Poisson equation:

$$\Delta V = -\frac{e}{\epsilon_0}(n_i - n_e - Q_d n_d), \tag{6}$$

$$\vec{E} = -\vec{\nabla}V, \tag{7}$$

where ϵ_0 is the permittivity of vacuum space, n_e is the electron density, n_i is the ion density, Q_d is the charge on a dust particle, and n_d is the dust density.

The electron energy density $w_e = n_e\epsilon$ (i.e., the product of the electron density and average electron energy ϵ) is calculated self-consistently from the second moment of the Boltzmann equation:

$$\frac{dw_e}{dt} + \vec{\nabla}\cdot\vec{\Gamma}_w = -e\vec{\Gamma}_e\cdot\vec{E} + S_w, \tag{8}$$

with $\vec{\Gamma}_w$ being the electron energy density flux,

$$\vec{\Gamma}_w = \frac{5}{3}\mu_e w_e\vec{E} - \frac{5}{3}D_e\vec{\nabla}w_e, \tag{9}$$

and μ_e and D_e are the electron mobility and electron diffusion coefficients. Term S_w in the electron energy balance equation is the loss of electron energy due to electron impact collisions, including excitation, ionization, and recombination of electrons on the dust particle's surface. To compute the sources as a function of ϵ, tables are generated using the two-term Boltzmann solver for the electron energy distribution function. Via the surface charge on the electrodes, the plasma can be connected to a resistance-inductance-capacitance (RLC) circuit. Further details about the algorithms used to solve the above mentioned equations can be found in Ref. [7].

B. Implementing dust as a fluid

1. Charging of dust

When a dust particle exceeds a certain size it can collect more than one electron and be charged up to the floating potential relative to the surrounding plasma. This potential depends on the local ion and electron density and energy distribution. For a spherical dust particle with radius r_d, much smaller than the linearized Debye length, the orbital-motion-limited theory [11] predicts a positive ion and electron current:

$$I_i = 4\pi r_d^2 e n_i \sqrt{\frac{k_B T_i}{2\pi m_i}}\left(1 - \frac{eV_{fl}}{k_B T_i}\right), \tag{10}$$

$$I_e = 4\pi r_d^2 e n_e \sqrt{\frac{k_B T_e}{2\pi m_e}}\exp\left(\frac{eV_{fl}}{k_B T_e}\right). \tag{11}$$

Here, n_e is the electron density, n_i is the positive ion density, e is the elementary charge, k_B is Boltzmann's constant, T_i is the positive ion temperature, T_e is the electron temperature, m_i is the ion mass, m_e is the electron mass, and V_{fl} is the floating potential. All species are assumed to have a Maxwellian energy distribution. The influence of neighboring dust particles is neglected.

When the ions enter the plasma sheaths near the electrodes, they get a directed velocity $\vec{v}_i$ due to the electric field. Therefore, we have replaced $k_B T_i$ in the expression for the ion current by the mean energy E_i, which is

$$E_i = \frac{4k_B T_{gas}}{\pi} + \frac{1}{2}m_i v_i^2. \tag{12}$$

Equation (12) is obtained by using the mean speed expression of Barnes *et al.* [13] given by

$$v_s = \left(\frac{8k_B T_{gas}}{\pi m_i} + v_i^2\right)^{1/2}. \tag{13}$$

By calculating $\frac{1}{2}m_i v_s^2$, Eq. (12) is obtained. The directed velocity v_i is the drift velocity of the ions [Eq. (2)].

In the model the charge $Q_d = 4\pi\epsilon_0 r_d V_f$ on the dust is calculated from the equilibrium of the currents in Eqs. (10) and (11).

The floating potential of the dust is assumed to be constant during a rf cycle. This assumption is justified by the fact that the currents towards the dust particle surface are too small to change the charge significantly during a rf cycle.

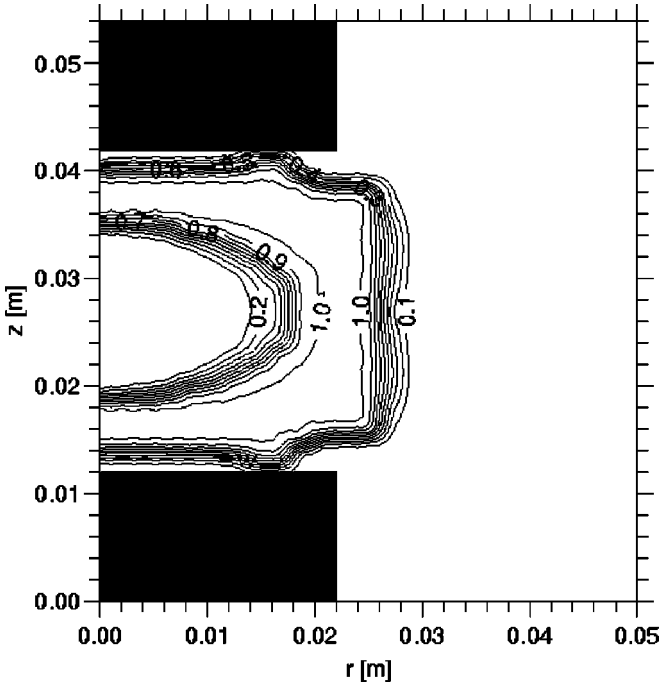

FIG. 2. Dust density profile in m^{-3}, normalized with a factor of 1.55×10^{10}.

2. Recombination on dust particles

When a dust particle becomes negatively charged, it will attract positive ions, these will recombine with an electron that has to be replaced again by an electron from the discharge to maintain the floating potential. As a result the equilibrium fluxes of positive ions and electrons arriving at the dust surface will recombine and the released energy is used to heat up the dust particle surface [9,10]. The electron flux [Eq. (11)] results in a recombination rate:

$$R=4\pi r_d^2 n_d n_e \sqrt{\frac{k_B T_e}{2\pi m_e}}\exp\left(\frac{eV_{fl}}{k_B T_e}\right). \tag{14}$$

3. Forces acting on a dust particle

In a plasma, dust particles undergo a wide variety of forces. Assuming that a dust particle is a perfect sphere, the gravitational force can be written as

$$\vec{F}_g=\tfrac{4}{3}\pi r_d^3 \rho_d \vec{g}, \tag{15}$$

where r_d is the dust particle radius, ρ_d is the mass density, and $\vec{g}$ is the gravitational acceleration. For the often used melamine-formaldehyde dust particle, ρ_d is approximately 1.51×10^3 kg/m^3.

When a dust particle has a velocity relative to the neutral gas, it will experience a drag force due to momentum transfer from (to) the gas. This neutral drag force has been discussed in detail by Graves *et al.* [12]. It can be approximated by

$$\vec{F}_n=-\tfrac{4}{3}\pi r_d^2 n_n(\vec{v}_d-\vec{v}_n)v_{th}m_n, \tag{16}$$

where n_n is the density of the neutral with mass m_n, $\vec{v}_d$ is the drift velocity of the dust particle, $\vec{v}_n$ is the velocity of the gas, and v_{th} is the average thermal velocity of the gas. Because advection of the neutral gas is not included in the model, $\vec{v}_n=\vec{0}$, this force will only be present as a damping force on the velocity of the dust particles.

Another force caused by momentum transfer is the ion drag. This force results from the positive ion current that is driven by the electric field. It consists of two components. The collection force represents the momentum transfer of all the ions that are collected by the dust particle and is given by

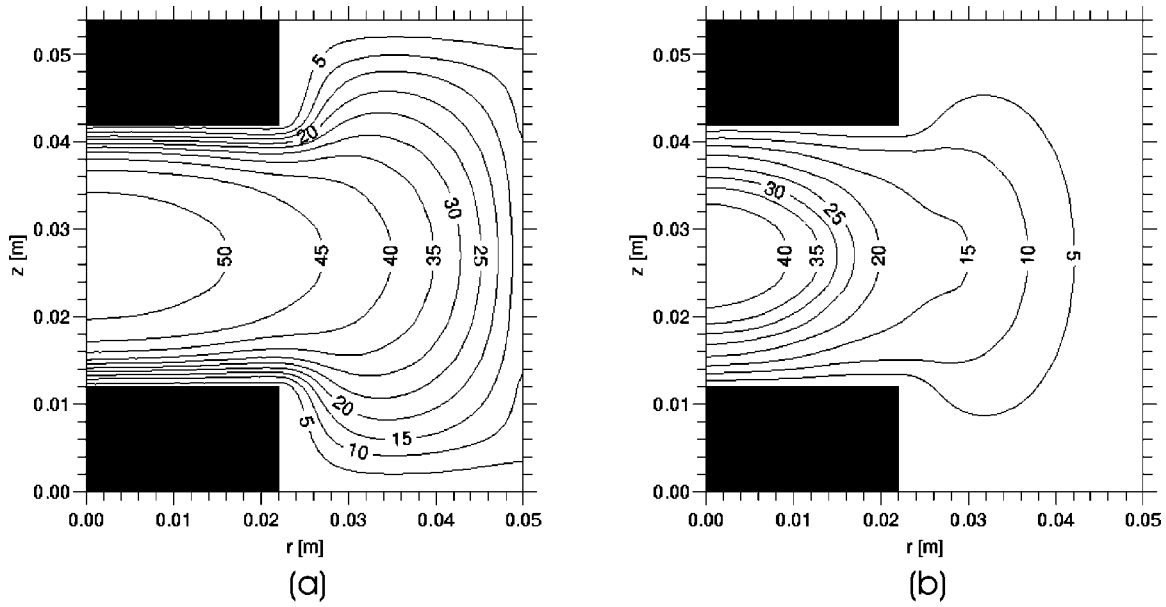

FIG. 3. Time-averaged electric potential in volts in dust-free discharge (a) and for a dusty argon discharge (b).

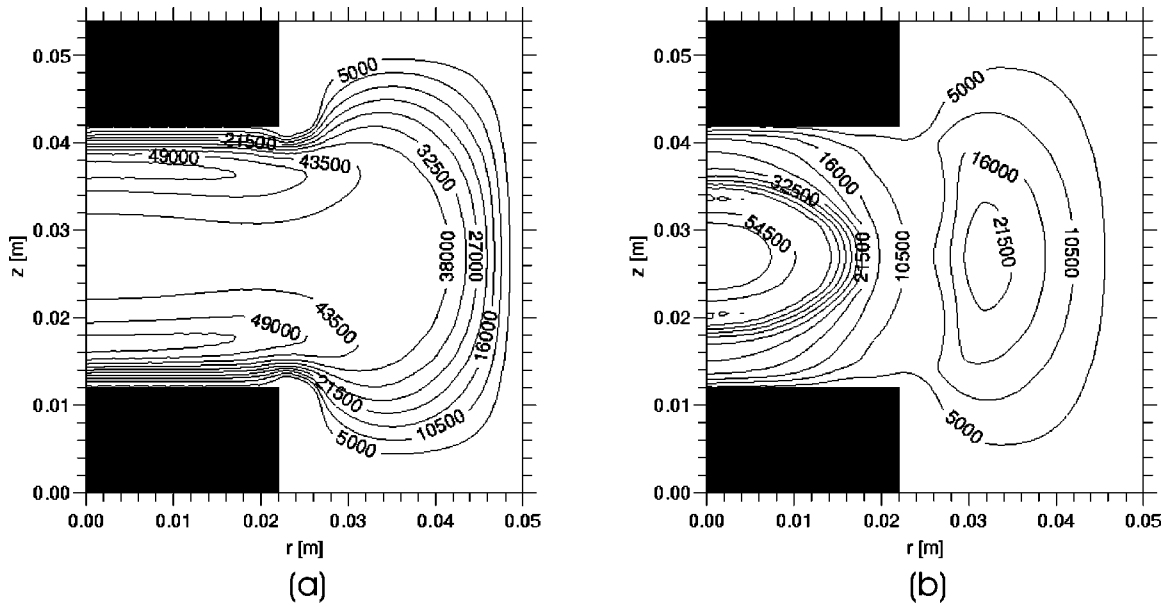

FIG. 4. Number of electrons on a dust particle with diameter of 15 μm in a dust-free discharge (a) and for a dusty argon discharge (b).

$$\vec{F}_i^c = \pi b_c^2 n_i v_s m_i \vec{v}_i , \tag{17}$$

where v_s is the mean speed of the ions, $\vec{v}_i$ is the ion drift velocity, and b_c is the collection impact parameter.

The second component is the orbit force given by

$$\vec{F}_i^o = 4\pi b_{\pi/2}^2 \Gamma n_i v_s m_i \vec{v}_i , \tag{18}$$

with $b_{\pi/2}$ being the impact parameter that corresponds to a deflection angle $\pi/2$ and Γ being the Coulomb logarithm,

$$\Gamma = \frac{1}{2}\ln\left(\frac{\lambda_L^2 + b_{\pi/2}^2}{b_c^2 + b_{\pi/2}^2}\right), \tag{19}$$

$\lambda_L = [(1/\lambda_e)^2 + (1/\lambda_i)^2]^{-1/2}$ is the linearized Debye length, which is a combination of the electron Debye length λ_e and the ion Debye length λ_i. The ion drag is discussed in more detail by Barnes *et al.* [13]. Previous calculations have shown that the ion drag should be enhanced by at least a factor 5 or the linearized Debye length in the Coulomb logarithm [Eq. (19)] should be replaced by the electron Debye length, in order to generate a void [3]. This factor is also included in the calculation presented here. Khrapak *et al.* [14] have studied cases where the ion drag force is underestimated by using the ion drag expression of Barnes. These cases are quite similar to ours. Lampe *et al.* [15] have shown that collisions with the background gas may enhance the

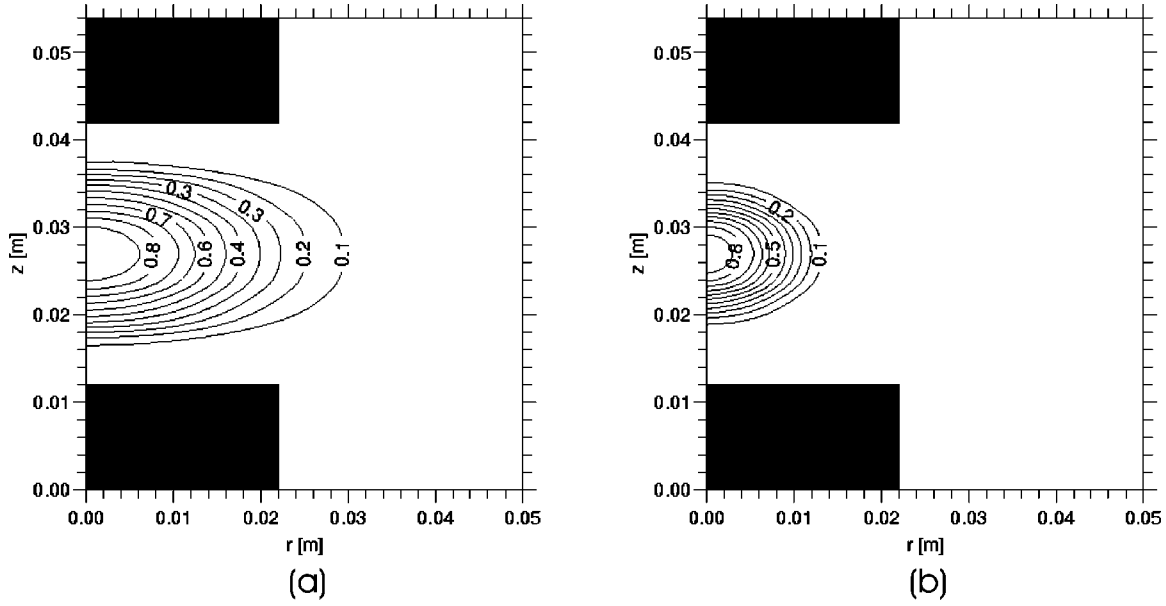

FIG. 5. Time-averaged electron density in m^{-3} for a dust-free discharge, normalized with a factor of 2.59×10^{15} (a) and for a dusty argon discharge, normalized with a factor of 2.61×10^{15} (b).

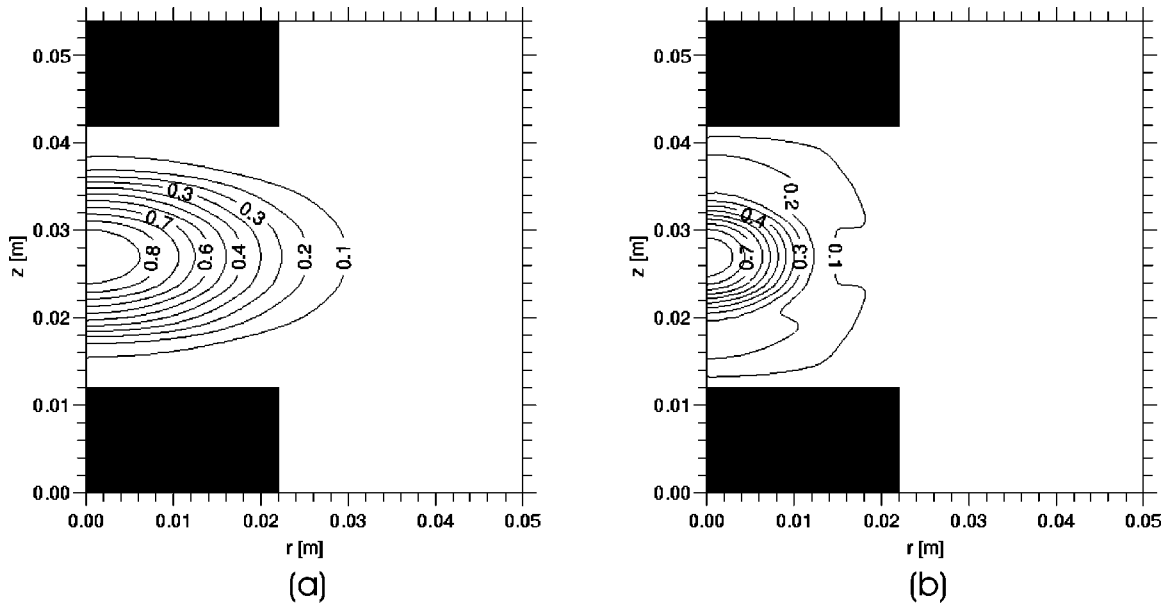

FIG. 6. Time-averaged ion density in m^{-3} for a dust-free discharge, normalized with a factor of 2.59×10^{15} (a) and for a dusty argon discharge, normalized with a factor of 2.61×10^{15} (b).

collection of ions. This could explain the factor 5 needed in our simulations.

Due to their charge, dust particles will experience an electric force. Daugherty *et al.* [16] derived the following expression:

$$\vec{F}_e = Q_d\vec{E}\underbrace{\left(1+\frac{\kappa r_d}{3(1+\kappa r_d)}\right)}_{\approx 1}, \tag{20}$$

where Q_d is the charge on the dust particle, $\vec{E}$ is the electric field, and $\kappa = 1/\lambda_L$. In a discharge, the dust particle radius is much smaller than the linearized Debye length, therefore the term within the bracket is approximately 1 and the electric force is given by

$$\vec{F}_e = Q_d\vec{E}. \tag{21}$$

This expression holds for situations where the dust particles are not shielded from the plasma by positive ions trapped in orbitals around the dust particle [15]. In that case the particle plus ion cloud will behave as some kind of dipole.

When a temperature gradient is present in a discharge, for instance, due to cooling or heating of the electrodes, a third force driven by momentum transfer will occur. This force is

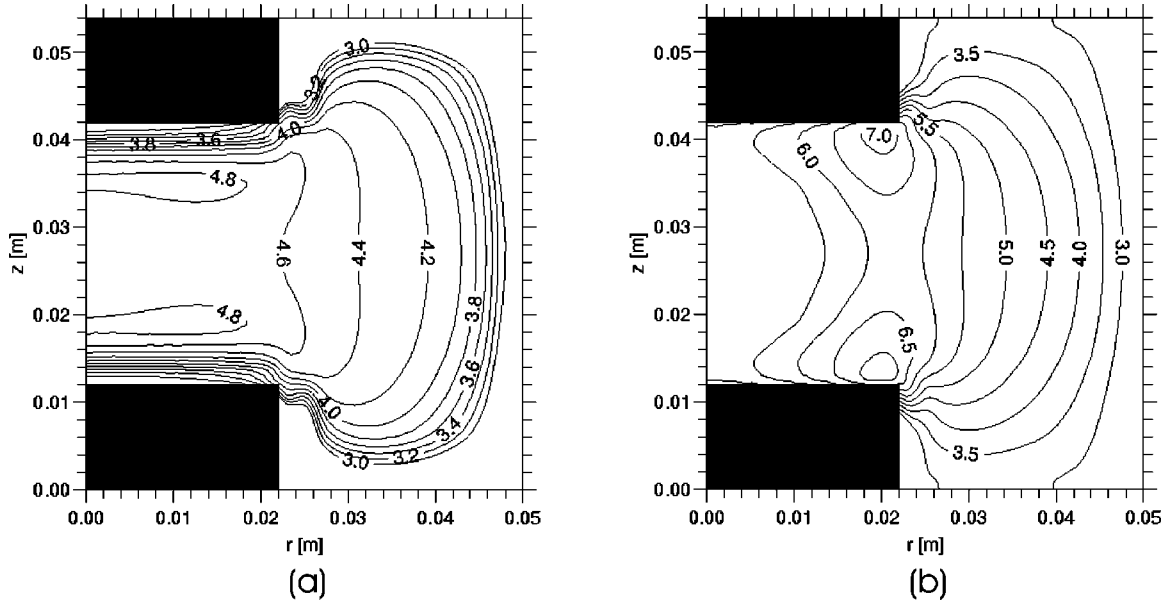

FIG. 7. Time-averaged electron energy in eV for a dust-free discharge (a) and for a dusty argon discharge (b).

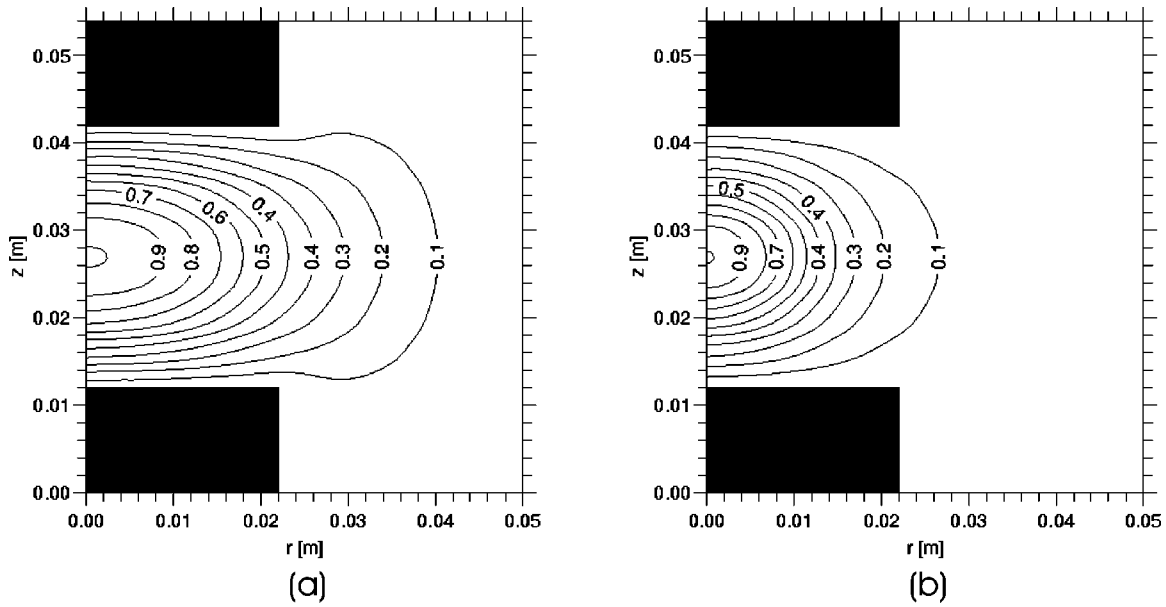

FIG. 8. Time-averaged argon metastable density in m^{-3} for a dust-free discharge, normalized with a factor of 4.01×10^{17} (a) and for a dusty argon discharge, normalized with a factor of 4.92×10^{17} (b).

called the thermophoretic force. Atoms impinging from the hot side have more momentum than their companions of the cold side, this can result in a force pointing in the direction $-\vec{\nabla}T$.

For large Knudsen numbers, Talbot *et al.* [17] derived the following expression:

$$\vec{F}_{th}=-\frac{32}{15}\frac{r_d^2}{v_{th}}\left(1+\frac{5\pi}{32}(1-\alpha)\right)\kappa_T\vec{\nabla}T, \tag{22}$$

$v_{th}=[8k_BT_{gas}/(\pi m)]^{1/2}$ is the average thermal velocity of the gas. κ_T is the translation part of the thermal conductivity. α, the thermal accommodation coefficient of the gas is taken equal to 1.

To obtain a suitable expression for the flux of dust particles, we assume that the neutral drag force is in equilibrium with the sum of the other forces. This assumption is valid when the final steady state is approached, but should be relaxed, for instance, when the dust is injected at a high velocity. In that case the inertia of the dust should not be neglected. With the introduction of a momentum loss frequency and a mobility and diffusion coefficient for the dust particles given by

$$\nu_{md}=\sqrt{2}\,\frac{p_{tot}}{k_BT_{gas}}\pi r_d^2\sqrt{\frac{8k_BT_{gas}}{\pi m_d}}, \tag{23}$$

where p_{tot} is the static pressure and m_d the dust particle's mass,

$$\mu_d=\frac{Q_d}{m_d\nu_{md}}, \tag{24}$$

$$D_d=\mu_d\frac{k_BT_{gas}}{Q_d}, \tag{25}$$

it is possible to define a ''drift-diffusion'' expression for the flux of the dust particles,

$$\vec{\Gamma}_d=-\mu_dn_d\vec{E}_{eff}-D_d\vec{\nabla}n_d-\frac{n_d}{\nu_{md}}\vec{g}+\frac{n_dm_iv_s}{m_d\nu_{md}}(4\pi b_{\pi/2}^2\Gamma+\pi b_c^2)\vec{\Gamma}_i-\frac{32}{15}\frac{n_dr_d^2}{m_d\nu_{md}v_{th}}\kappa_T\vec{\nabla}T, \tag{26}$$

and treat them with the same numerical procedures as the other charged particles in the fluid model. Because of the low mobility of the dust particles the effective field $\vec{E}_{eff}$ is approximated by the time-averaged rf field. The diffusion originates from the pressure gradient, $k_BT_d\vec{\nabla}n_d$. The Einstein relation couples the diffusion and the mobility coefficients, see Eq. (25).

The drift velocity and the diffusion coefficient of the dust fluids are much smaller than those of the ions and electrons. Therefore it would require a large computational effort to achieve a steady state solution for the dust when it is followed during a rf cycle. We, therefore, have developed a method to speed up the convergence toward the steady state solution by introducing a different calculation cycle with a different time step for the dust. Our model thus consists of two calculation cycles. In the first, the transport equations of the ions, electrons, and the Poisson equation are solved during a number of rf cycles; during the rf cycles the dust does not move. After that, the transport equation of the dust is solved with a greater time step, using the time-averaged electric field, and electron and positive ion fluxes. During the second calculation, space charge regions are created, because the electron and positive ion densities do not change. These

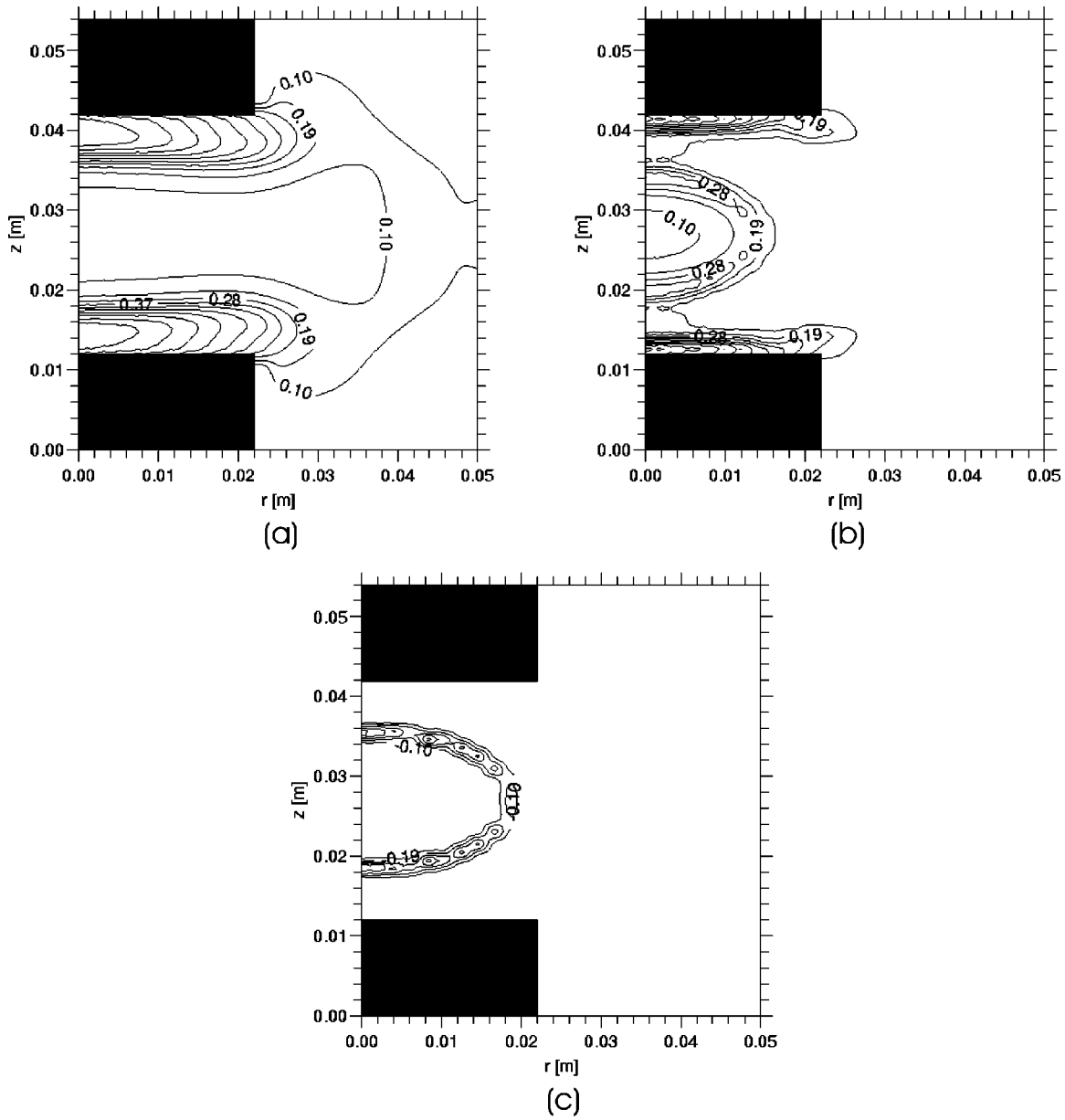

FIG. 9. (a) Time-averaged net space charge in m^{-3} for a dust-free argon discharge in elementary charges, normalized with a factor of 1.42×10^{14}. (b) Time-averaged positive space charge in m^{-3} for a dusty argon discharge in elementary charges, normalized with a factor of 2.16×10^{14}. (c) Time-averaged negative space charge in m^{-3} for a dusty argon discharge in elementary charges, normalized with a factor of 5.78×10^{13}.

space charge regions will lead to instabilities in the solution of the Poisson equation and the electron transport. To solve this problem, we correct the artificially generated space charge by adapting the positive ion density distributions prior to the next series of rf cycles, in which the ion and electron density profiles adapt themselves to the new dust density profile. With this method the required speed-up is established. Both for the plasma species and for the dust fluids the transport equations are solved using the Sharfetter-Gummel exponential scheme [7]. To model the reactor (Fig. 1), we have used a grid of 24 radial gridpoints times 48 axial gridpoints. We make use of a nonequidistant grid. The radial spatial resolution is 0.21 cm and the axial resolution between the electrodes is 0.09 cm. More details about the used discretion schemes can be found in Ref. [7].

The internal pressure of the crystal due to the interparticle interaction has been included by means of a density dependence of the diffusion coefficient for the dust. The diffusion coefficient of the dust is increased by a factor $\exp(N_d/N_c)$, where the reference density N_c is chosen such that the dust density saturates at a value N_{crys}. This models the incompressibility of the crystal. Actually, the (yet unknown) equation of state of the dust crystal should be used to account for the internal pressure. Since we were not primarily interested in the precise structure of the crystallized regions, we have chosen for the simple and computationally robust exponential increase of D_d. Plasma crystal experiments [1] have shown an interparticle distance of about 300 μm for a dust

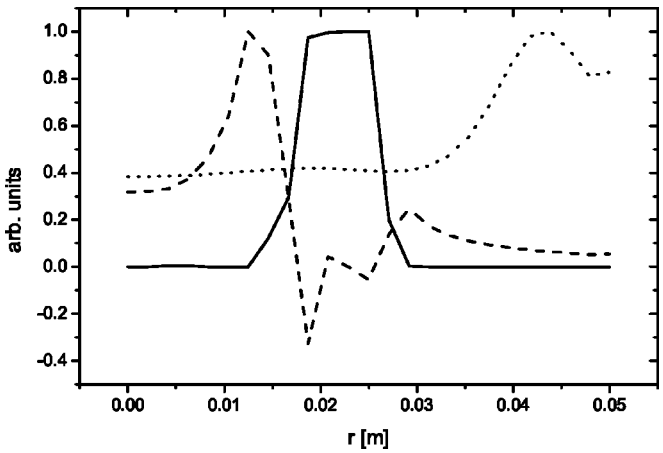

FIG. 10. Dust density profile and the net space charge profile for a dust-free and a dusty argon discharge at the axial symmetry axis. The thick curve represents dust density profile of the 15-μm-sized dust particles, normalized with a factor of 1.48×10^{10}. The dashed curve represents the net space charge in a dusty argon discharge, normalized with a factor of 5.37×10^{13}. The dotted curve represents the net space charge for a dust-free discharge at the axial symmetry axis, normalized with a factor of 1.84×10^{13}.

particle of 15 μm diameter. This results in an average ''crystal'' density N_{crys} of 3.7×10^{10} m^{-3}.

III. RESULTS AND DISCUSSION

In this section, the results obtained with the two-dimensional argon-dust fluid model are presented. The PKE chamber used by Morfill *et al.* has been modeled (Fig. 1). The reactor is cylindrically symmetric. The simulation starts with a zero dust density profile. During the simulation the dust is injected from both electrodes by adding source terms in the dust particle balances for the first grid points below (above) the electrodes. The injection rate is about 250 000 particles per second. Eventually a total amount of 0.7×10^{6} dust particles is reached, after that the sources are switched off. Both electrodes are driven by a radio-frequency power source at a frequency of 13.56 MHz. The peak-to-peak voltage is 70 V, this results in a power dissipation of about 0.04 W. The pressure is 40 Pa. The dust particles have a diameter of 15 μm. Comparisons of the plasma parameters are made for a dusty and a dust-free argon discharge.

Figure 2 shows the steady state dust density profile. In the center of the discharge, a dust-free region, the so-called void, appears, surrounded by a crystalline region of dust with an average density of 1.55×10^{10} m^{-3}. This gives an interparticle distance of about 400 μm.

Figures 3(a) and 3(b) show the time-averaged potential distribution $V(r,z)$ in the dust-free and dusty argon discharges. In both cases the potential has its maximum in the bulk of the plasma between the electrodes. Comparing the potential distributions, a significant change in the plasma potential can be observed. The plasma potential in the center of the dusty discharge has decreased compared with the dust-free case. This shows the importance of taking into account both the contribution of the charge on the dust [Figs. 4(a) and 4(b)] in the Poisson equation and the recombination on the dust particle surface. It can also be seen that if a dust particle would settle in the center of the discharge it would get a higher charge in a dusty discharge. This is mainly due to a higher electron energy. The nonuniform charge distribution is the result of the spatial distribution of the ions, electrons, and electron energy. The enhanced ion density in the dust cloud reduces the dust charge.

Comparing Figs. 5(a) and 5(b), it can be seen that indeed the recombination on the dust particle surface acts as a sink for the electrons. The same is observed for the argon ions [Figs. 6(a) and 6(b)]. Due to a decrease in the electron and ion densities, the remaining electrons can gain more energy from the larger oscillating electric field, this gives rise to a

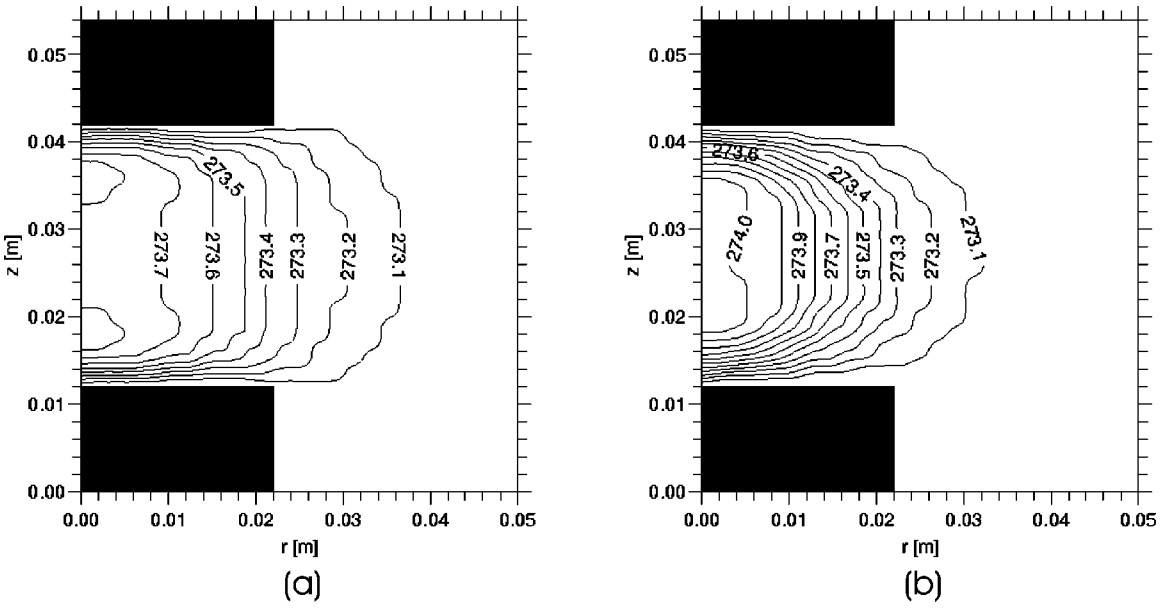

FIG. 11. Gas temperature in Kelvin for a dust-free discharge (a) and for a dusty argon discharge (b).

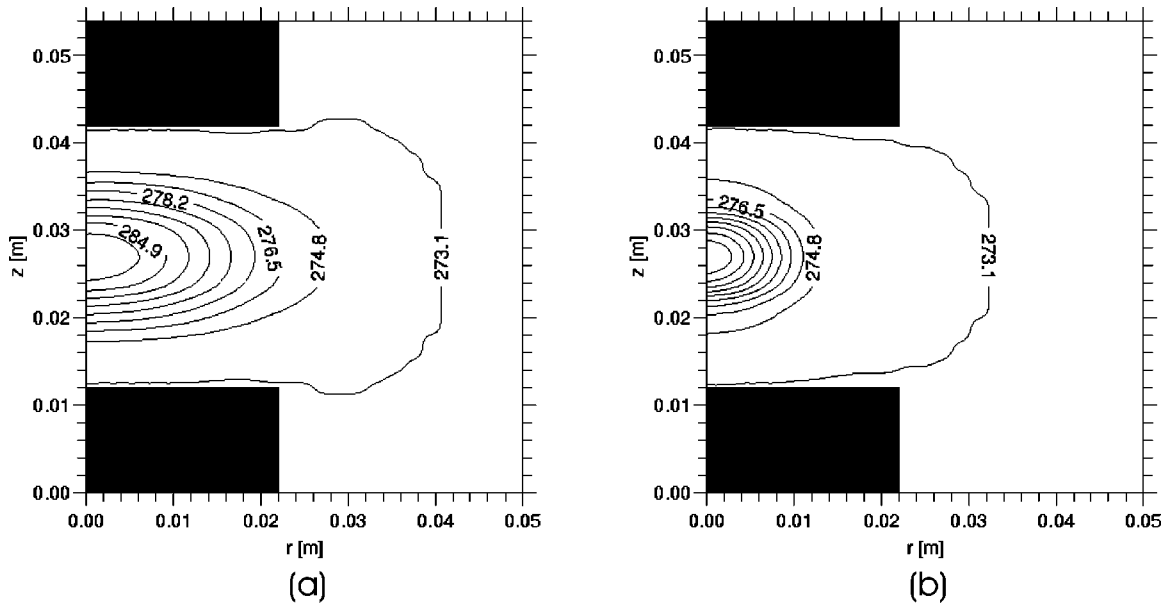

FIG. 12. Dust particle surface temperature in Kelvin for a dust-free discharge (a) and for a dusty argon discharge (b).

higher electron temperature in a dusty discharge [Figs. 7(a) and 7(b)]. This increase in electron temperature enhances the production of the argon metastables by almost 25%. This is shown in Figs. 8(a) and 8(b). In the experiments the enhanced electron temperature is seen via an increase in the intensity of the light emitted from inside the void due to excited argon atoms. However, the metastables density could be used as an indirect indicator for the light emerging from the void.

Figure 9(a) shows the net space charge in a dust-free argon plasma. As expected, positive space charge regions appear only close to the electrodes and the reactor wall. At the center between the electrodes, a quasineutral region can be observed. For the dusty discharge case an interesting phenomenon can be observed. Figures 9(b), 9(c), and 10 show a double space charge layer that appears around the sharp boundary of the dust crystal. This double space charge layer inside the void has been described by Annaratone *et al.* [18]. The positive space charge layer in front of the dust crystal boundary is caused by the recombination on the dust particle's surfaces of ions and electrons entering the crystal. As in front of an absorbing wall, the difference in mobility between the ions and the electrons results in a net positive space charge that enhances the electric field, which, in turn, accelerates the ions from the center of the void towards the dust crystal to compensate for the mobility difference. The negative space charge region appears very close to the sharp edges inside the dust crystal. It appears due to the fact that the diffusion of the argon ions prohibits a full compensation of the fast rising negative charge of the dust crystal. These double space charge layers could explain the repulsion effect of the generated dust clouds during the first stages of injection, which slows down the mixing of the dust clouds seen in the PKE experiments [1].

Figures 11(a) and 11(b) show the gas temperature for the dust-free and dusty discharges. The gas temperature profile in a dusty plasma has two maxima of 274.1 K in the sheaths, which is about 1 K higher than the reactor wall temperature that is kept at 273 K. In Figs. 12(a) and 12(b) the dust particle (surface) temperature is shown for the dust-free and dusty discharges; it can be observed that a dust particle would get a maximum temperature in the center of the plasma if it would settle there. This is due to the maximum in the ion and electron densities in the middle of the discharge, giving a maximum recombination energy flux towards the dust particles surface. Note that the difference between the gas and dust particle surface temperature is about 9 K at the center of the discharge. Comparing the gas temperatures for a dust-free and a dusty discharge [Figs. 11(a) and 11(b)] shows that the effect of the dust on the gas temperature profile is negligible.

IV. CONCLUSIONS

The numerical simulation results show that self-consistent modeling of the plasma parameters in a dusty argon discharge is important. Both the contribution of the charge on the dust in the Poisson equation and the recombination on the dust particle surface must be taken into account. Recombination on the dust particle's surface results, for instance, in a significant difference in electron and ion densities between a dust-free and a dusty argon discharge. Also the other plasma parameters are affected, such as the electron temperature, the electric potential, and the charge on the dust particles. An interesting phenomenon is the appearance of a double space charge at the edge of the dust crystal, which is formed by the difference in mobility between the ions and electrons and the diffusive transport of the ions caused by the steep density gradients. The modeling results also show an increase in the density of the argon metastables inside the void, illustrating in an indirect way the increased light emis-

sion emerging from the void due to excited argon atoms, as observed in the PKE experiments [1].

ACKNOWLEDGMENTS

The authors gratefully acknowledge the invaluable discussions with Professor J. Goree (University of Iowa), Professor G. Morfill, Dr. H. Thomas, Dr. B.M. Annaratone, and Dr. A.V. Ivlev (MPI für Extraterrestische Physik, Garching). This work was performed under the Euratom-FOM Association Agreement with financial support from the Netherlands Organization for Scientific Research (NWO), the Netherlands Organization for Energy and the Environment (NOVEM), and Euratom.

[1] G.E. Morfill *et al.*, Phys. Rev. Lett. **83**, 1598 (1999).
[2] H. Thomas *et al.*, Phys. Rev. Lett. **73**, 652 (1994).
[3] M.R. Akdim *et al.*, Phys. Rev. E **65**, 015401(R) (2002).
[4] T. Nitter, Plasma Sources Sci. Technol. **5**, 93 (1996).
[5] P. Belenguer *et al.*, Phys. Rev. A **46**, 7923 (1992).
[6] V. Vyas *et al.*, J. Appl. Phys. **92**, 6451 (2002).
[7] J.D.P. Passchier *et al.*, J. Appl. Phys. **73**, 1073 (1993).
[8] I. Revel *et al.*, J. Appl. Phys. **88**, 2234 (2000).
[9] M.R. Akdim *et al.*, Phys. Rev. E **67**, 056405 (2003).
[10] G.H.P.M. Swinkels *et al.*, J. Appl. Phys. **88**, 1747 (2000).
[11] J.E. Allen *et al.*, J. Plasma Phys. **63**, 299 (2000).
[12] D.B. Graves *et al.*, Plasma Sources Sci. Technol. **3**, 433 (1994).
[13] M.S. Barnes *et al.*, Phys. Rev. Lett. **68**, 313 (1992).
[14] S.A. Khrapak *et al.*, Phys. Rev. E **66**, 046414 (2002).
[15] M. Lampe *et al.*, Phys. Rev. Lett. **86**, 5278 (2001).
[16] J.E. Daugherty *et al.*, J. Appl. Phys. **73**, 1617 (1994).
[17] L. Talbot *et al.*, J. Fluid Mech. **101**, 737 (1980).
[18] B.M. Annaratone *et al.*, Phys. Rev. E **66**, 056411 (2002).